

Laser-Printed and Processed LiCoO₂ Cathode Thick Films for Li-Ion Microbatteries

Heungsoo KIM^{*1}, Johannes PROELL^{*2}, Robert KOHLER^{*2}, Wilhelm PFLEGING^{*2,3}, and Alberto PIQUE^{*1}

^{*1} *1-Naval Research Laboratory, Washington DC, 20375, U.S.A*

E-mail: heungsoo.kim@nrl.navy.mil

^{*2} *2- Karlsruhe Institute of Technology, IAM-AWP, P.O. Box 3640, 76021 Karlsruhe, Germany*

^{*3} *3- Karlsruhe Nano Micro Facility, H.-von-Helmholtz-Platz 1, 76344 Egg.-Leopoldshafen, Germany*

Thick-film electrodes (LiCoO₂ cathode and carbon anode) are laser-printed onto metallic current collectors for fabricating Li-ion microbatteries. Microbatteries fabricated with these laser-printed thick-film electrodes demonstrate a significantly higher discharge capacity and power density than those made by sputter-deposited thin-film techniques. This increased performance is attributed to the porous structure of the laser-printed electrodes that allows improved ionic and electronic transport through the thick electrodes (up to ~100 μm) without a significant increase in internal resistance. Laser structuring process is applied to increase active surface area of the laser-printed LiCoO₂ cathode films for improving cycle stability of microbatteries at high charging/discharging currents. Laser structuring parameters, including laser pulse number and laser fluence, are optimized for improving surface morphology of the films.

DOI:10.2961/jlmn.2012.03.0016

Keywords: Thick-film electrodes, Li-ion microbatteries, Laser direct-write, Laser structuring, 3D battery

1. Introduction

In recent years, there is a strong demand for miniaturized rechargeable power sources for autonomous microelectronic devices such as wireless network microsensors. Thin-film Li and Li-ion microbatteries are being studied as a current-state-of-the-art micropower source due to their high operating voltages, high energy densities and long cycle life [1-3]. To date, these rechargeable thin-film microbatteries have been prepared by physical deposition methods, such as sputtering [1-3], pulsed laser deposition (PLD) [4], chemical vapor deposition [5], and sol-gel [6] techniques. Among these, the sputtering techniques have been widely utilized because they can grow all battery components including cathode electrodes (lithium-transition metal oxides), anode electrodes (Li-metal), electrolyte/separator (commonly lithium phosphorous oxynitride, LIPON), and current collectors (Al or Cu). However, the sputtering techniques are not able to deposit traditional composite components (active material, carbon and electrolyte) simultaneously, indicating that sputter-deposited cathode thin films (e.g. LiCoO₂) provide relatively small conductivity because of no conducting carbon in the films. In this matter, the thicknesses of the cathode films prepared by the sputtering techniques are typically limited to 1 to 5 μm in order to keep cell resistance low. Dudney and Jang demonstrate that Li-LiCoO₂ solid-state thin-film microbatteries with a cathode thickness of 1 μm deliver as much as ~95 % of the maximum capacity, whereas the batteries with a 5 μm-thick cathode supply only 75 % of the maximum capacity [2]. The discharge capacity of the thicker LiCoO₂ cathode films decreases more rapidly with increasing dis-

charge current density [2]. This is attributed to the relatively high internal cell resistance of the thicker, less conducting cathodes, which limits the diffusivity of lithium ions. Because of this thickness limitation, the power and capacity per active electrode area of the thin-film microbatteries are not sufficient to operate many microelectronic devices.

In order to overcome the thickness limitation (i.e., low power and energy density) in thin-film microbatteries, the laser printing technique, which is a laser direct write (LDW) process, is used to develop thick-film electrodes. LDW allows for the fabrication of highly porous structured thick-film electrodes [7-10] without the use of any lithographic patterning steps. In LDW, a laser pulse is used to transfer or print 3-D pixels or voxels of an ink or paste containing a suspension of the electrode materials onto a substrate in order to form a pattern. Processing can convert the laser-printed patterns into a porous thick-film structure ideally suited for microbattery applications. Laser-printed electrodes could provide much higher capacities per electrode area than the sputter-deposited thin-film electrodes, since their porous structure allows better ionic and electronic transport through the thick electrodes (~100 μm) without a significant internal resistance. The LDW technique also can directly embed the electrochemical component into the substrates, reducing the size and weight of the microdevices [11]. Furthermore, this process can be combined with *in situ* laser annealing for processing the layers of active materials without damaging the substrate underneath, which is ideally suited for developing power sources on flexible plastic substrates [12]. This LDW technique has successfully fabricated Li- and Li-ion microbatteries using

LiCoO₂ cathodes, carbon or Li anodes, and laser-transferable polymer-ionic liquid separator/electrolytes and liquid electrolytes [10,11,13]. In this study, we demonstrate an order of magnitude higher discharge capacities for Li-ion microbatteries fabricated with gel polymer electrolytes and much thicker electrodes (25 – 105 μm).

Three dimensional battery architectures have been proposed to enhance the power density while maintaining high energy density of micro-battery systems [14-16]. Applications of 3D-batteries include smart card devices, radio-frequency identification (RFID) chips and microelectromechanical systems (MEMS) and micro-spacecraft [17-19]. As manufacturing process of the 3D architectures substrate structuring, usually silicon, has been discussed [20, 21]. Very recently, laser structuring processes for thin films have been developed allowing the formation of micro-structures directly out of the active electrode material such as lithium cobalt oxide (LiCoO₂) [22], lithium manganese oxide [23] and tin oxide [24]. For LiCoO₂ thin films created via magnetron sputtering and also for commercially available LiCoO₂ tape cast electrodes, the occurrence of laser-induced self-organizing surface structures has been reported [22,25].

In this paper, we detail the high discharge capacity of Li-ion microbatteries, fabricated using laser-printed thick-film electrodes (LiCoO₂ cathode and carbon anode). The influence of electrode thickness on the battery performance is then studied. High discharge capacities of ~2.4 mAh/cm² are demonstrated with thick LiCoO₂ cathodes (~105 μm). The performance of the thick-film Li-ion microbatteries is also compared with those results reported in the literature for microbatteries prepared by sputter-deposited thin-film electrodes. Finally, these laser-printed LiCoO₂ thick films are further treated with laser structuring process for increasing active surface area and improved capacity retention is observed for the batteries fabricated with the laser structured films.

2. Experimental

2.1 Electrode Materials

The cathode ink is formulated by mixing 91% LiCoO₂ (CO22, Seimi), 4% graphite (KS6, Timcal), 2% carbon black (Super P, Erachem) in a solution of 3% PVdF-HFP (Kynar 2801, Elf Atochem) in dibasic ester (DBE, a blend comprised of 59 wt. % dimethyl glutarate, 21 wt. %, dimethyl adipate, and 20 wt. % dimethyl succinate, Du Pont) solvent. The anode ink is prepared by mixing 91% carbon (MCMB 2528, Osaka Gas; MCMB stands for mesocarbon microbeads), 1% carbon black, and 8% PVdF-HFP in DBE solvent. In the electrode formulation, the graphite (KS6) is added to improve the electric conductivity and the carbon black (Super P) is added to increase porosity in the electrode films. The PVDF-HFP is used as a binder to hold the electrode films onto current collectors. The DBE is selected because it is a good solvent for PVDF binder and its boiling temperature is relatively high (~210 °C). The cathode and anode electrodes are laser-printed onto 50 μm thick Al and Cu current collectors, respectively.

2.2 Laser Printing Process

Figure 1 shows a schematic diagram of the LDW process used to print electrode materials in this work. Details of the LDW process has been described elsewhere [7-10]. Briefly, a small amount of electrode ink is cast as a uniform layer onto a 7.5 cm diameter UV transparent quartz wafer using a wire coater (#5, Garner) to form ~5 μm thick coating. The ink coated side of the quartz wafer (referred to as the “ribbon”) was placed above the receiving substrates (50 μm thick Al or Cu current collectors) on the X-Y stage at a distance of ~150 μm. Both the ribbon and the receiving substrate were translated by means of an X-Y motion control system (Aerotech, A3200).

A frequency-tripled Nd:YVO₄ (Spectra-Physics YHP40-355) pulsed laser (355 nm) operating at 10 kHz was switched in amplitude and time by an acousto-optic modulator (AOM) to provide up to a few hundred μJ of pulse energy. The laser beam was then expanded to fill a square aperture (560 μm x 560 μm), which was then imaged through a 10X objective to produce a 55 x 55 μm² spot. A CCD camera positioned to view along the same optical axis as the focusing objective provided a real-time plan view of the transfer process and sample.

The laser fluence is maintained at ~50 – 100 mJ/cm², while the number of transfer passes is varied to control the transferred film thickness. The laser-printed electrodes are dried in a vacuum oven at 120 °C for 24 hrs in order to remove the DBE solvent and any absorbed water. The dried electrodes are then transferred to a glove box (Ar, O₂ and H₂O < 1 ppm) and stored for 24 hrs prior to assembly, allowing the absorbed oxygen and moisture in the electrodes to equilibrate with the levels of the glove box.

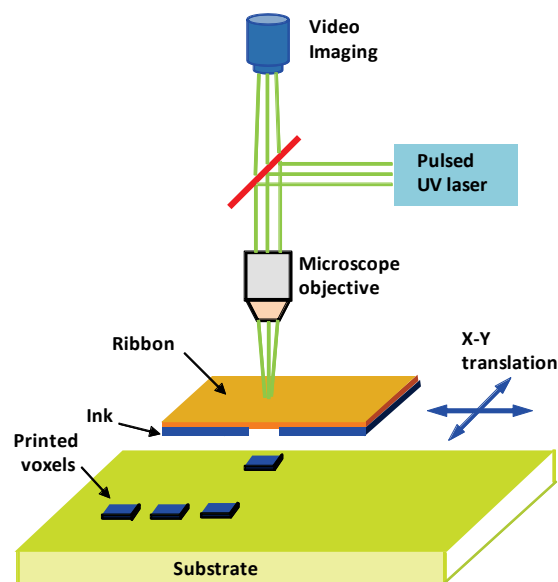


Fig. 1. A schematic diagram of the LDW system.

2.3 Battery Assembly and Characterization

In order to avoid electrolyte leakage problem during battery assembly, the gel polymer electrolytes (GPEs) are used in this work by mixing a polymer matrix and a liquid

electrolyte. PVdF-HFP is used as the polymer matrix for the GPE. A solution of 1 M LiPF_6 (Aldrich) in propylene carbonate (PC)/ethylene carbonate (EC)/dimethyl carbonate (DMC) (1:1:3 by volume, used as received from Aldrich) is used as a liquid electrolyte. PVdF-HFP powder is dissolved into the liquid electrolyte solution by stirring at 60°C. A polyolefin based microporous membrane (E25MMS SETELA, Tonen Chemical Corp.) is used as a separator. The 25 μm thick membrane is immersed in the GPE solution for 20 min inside the glove box.

The active area of the printed electrodes is 0.49 cm^2 . The current collectors are cut out to 1.3 cm x 1.3 cm using a laser. The Li-ion microbatteries used for this work are assembled by placing the GPE soaked porous membrane between the LiCoO_2 cathode and the MCMB anode. In order to package the stacked assembly, the current collectors are sealed together with a thermally curable polymer spacer (Surlyn SF-71, Flex-O-Glass) placed along each edge of the active electrode area (7 mm x 7 mm). The sealing is performed by hot pressing the thermally curable polymer at $\sim 100^\circ\text{C}$ for 10 sec and then followed by immediate cold pressing in order to avoid the crystallization of the sealing polymer, which could result in pinhole leaks in the seal. Figure 2 shows a cross sectional schematic diagram of an assembled Li-ion microbattery. Microbatteries are cycled between 4.2 V and 3 V at a constant current of 100 $\mu\text{A}/\text{cm}^2$ using an Arbin battery tester (BT2000, Arbin Instruments) with MITS Pro 3.0 software.

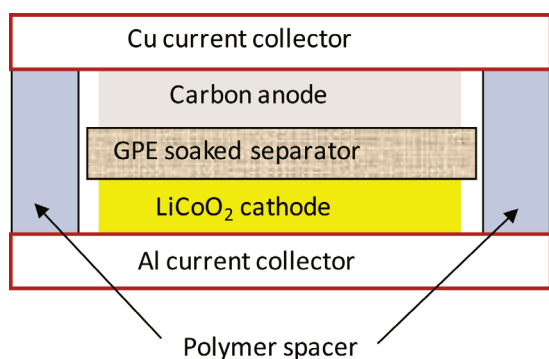


Fig.2. Cross-sectional schematic diagram (not to scale) of a typical Li-ion microbattery used in this research.

2.4 Laser Structuring and battery characterization

Figure 3(a) shows a schematic diagram of the laser structuring system used in this work. Laser patterning and surface modification is performed using a KrF-excimer laser (ATLEX-500-SI, ATL Laser-technik) operating at a wavelength of 248 nm. The laser pulse length is 5 ns (FWHM). The laser beam with a flat-top profile is projected onto the sample surface using a demagnifying lens (demagnification factor 10:1) with a numerical aperture of 0.4. Scanning electron microscope (SEM) images are taken with a XL30S (Philips) under an angle of 45° .

Electrochemical characterization of the laser structured LiCoO_2 cathode films is performed using Swagelok® cells and an Arbin Instruments BT2000 battery testing system. Figure 3(b) illustrates a Swagelok® cell used in this work. The Swagelok holders (product number: SS-12M0-6) are

made of stainless steel with an inner diameter of 12 mm. The plungers are also made of stainless steel with a diameter of 12 mm. The sealing rings are made of PTFE and a GF/A separator (thickness 260 μm , Whatman) is applied between the cathode and anode films. The metallic lithium foil (thickness 350 μm , Sigma Aldrich) is used as anode material and pressed onto a nickel substrate (thickness 500 μm) in order to achieve good electrical contact. A spring is inserted between the nickel substrate and the plunger in order to achieve a constant and reproducible mechanical force of 18.80 N. The electrolyte is conventional ethylene carbonate / dimethyl carbonate electrolyte containing 1M LiPF_6 . For laser structuring test and also Swagelok cell test, current collectors are cut out to 12 mm in diameter and the active area of LiCoO_2 electrodes is 0.785 cm^2 . Battery cycling is performed at a constant current between 3.0 V and 4.2 V. The applied current corresponds to a C-rate of C/5, when assuming a theoretical capacity of 140 mAh/g. A “C/5” rate means that the discharge current will discharge the entire battery in 5 hours.

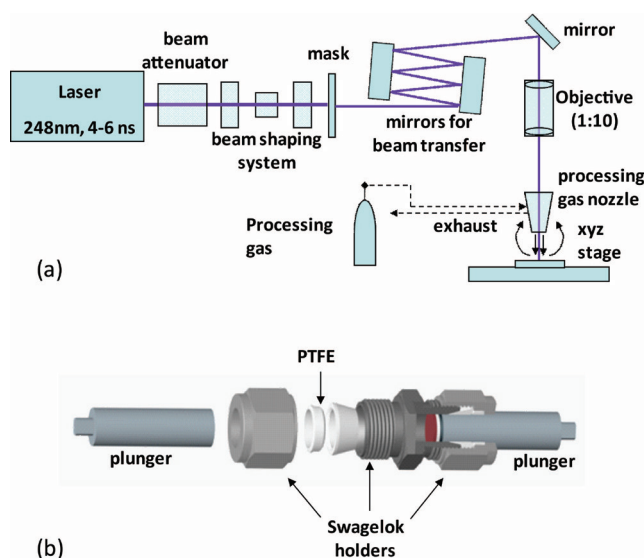


Fig.3. (a) A schematic illustration of the laser structuring system. (b) a schematic illustration of the Swagelok cell design.

3. Results and Discussion

3.1 Laser-printed thick-film electrodes

Figure 4 shows SEM images from the laser printed cathode (LiCoO_2 + graphite + carbon black) and anode (MCMB 2528 + carbon black) layers. The agglomerated LiCoO_2 powder grains mixed with the much smaller graphite and carbon black are clearly seen in Fig. 4(a), while the MCMB 2528 spherical particles mixed with the smaller carbon black can be observed in Fig. 4(b). Both SEM images also show the highly porous structure of both layers. This high porous structure allows improved ionic and electronic transport without a significant increase in cell internal resistance. Figure 4(c) shows a cross sectional SEM image of a packaged Li-ion battery. It is clear that each layer exhibits homogeneous structure with uniform thick-

ness, suggesting reduced safety hazards that maybe resulted from a consequence of overpotentials, local decomposition of electrolyte, and/or gas evolution.

The thickness and mass of the laser-printed electrode are easily controlled by the number of LDW transfer passes. For example, the 25 μm -thick LiCoO_2 cathode film is obtained after 6 LDW passes (6x) and the 52 μm -thick cathode film is achieved after 12 LDW passes (12x). The film thickness is also controlled by the ink viscosity, i.e., the solids content, used for the laser printing. For high viscosity inks, fewer LDW passes are needed to achieve the same film thickness obtained with low viscosity inks. In the case of high viscosity inks, however, a higher laser power must be utilized to transfer the inks, which might affect the quality of the transfers.

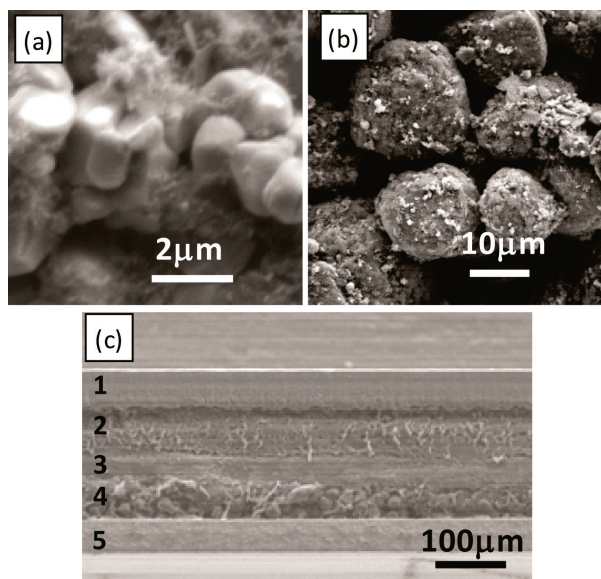


Fig. 4. SEM images of laser-printed (a) LiCoO_2 cathode and (b) carbon (MCMB2528) anode. (c) Cross-sectional SEM image of a packaged Li-ion battery. The layers from top to bottom are: 1) Al current collector, 2) LiCoO_2 cathode, 3) separator, 4) carbon anode and 5) Cu current collectors.

Figure 5 shows discharge curves for the 5th cycle for packaged Li-ion microbatteries with LiCoO_2 cathodes of different thicknesses (25 – 105 μm). The batteries were charged and discharged at a constant current of 100 $\mu\text{A}/\text{cm}^2$. The achieved discharge capacity per active cathode area is proportional to the cathode thickness. The discharge capacity at the 5th cycle increases from 600 to 2360 $\mu\text{Ah}/\text{cm}^2$ as the cathode thickness is increased from 25 to 105 μm . However, the specific discharge capacity per active cathode mass is slightly reduced with increasing electrode thickness due to a slightly increased internal resistance. The coulombic efficiency of all the batteries becomes greater than 98% and stays almost constant for the rest of the following cycles.

The battery performance of the laser-printed thick-film electrode microbatteries is compared against that of microbatteries fabricated with sputter-deposited thin-film electrodes. For example, Li-microbatteries with sputter-deposited 2.5 μm thick LiCoO_2 cathodes (active area = 1

cm^2) display capacities of $\sim 160 \mu\text{Ah}/\text{cm}^2$ (or $\sim 64 \mu\text{Ah}/\mu\text{m}\text{-cm}^2$) at a current density of 100 $\mu\text{A}/\text{cm}^2$ [1]. In this work, the Li-ion microbattery with a laser-printed 105 μm thick LiCoO_2 (active area = 0.49 cm^2) provided a capacity of $\sim 2360 \mu\text{Ah}/\text{cm}^2$ (or $\sim 22.5 \mu\text{Ah}/\mu\text{m}\text{-cm}^2$) at the same current density of 100 $\mu\text{A}/\text{cm}^2$. Even though the volumetric capacity is 3 times lower than that of the sputter-deposited thin-film cells, the laser-printed thick-film microbatteries can provide an order of magnitude higher discharge capacities per unit area. From this comparison, it is clear that laser-printed thick-film microbatteries are well suited for applications requiring not only high discharge capacity but also limited cell footprints due to size constraints.

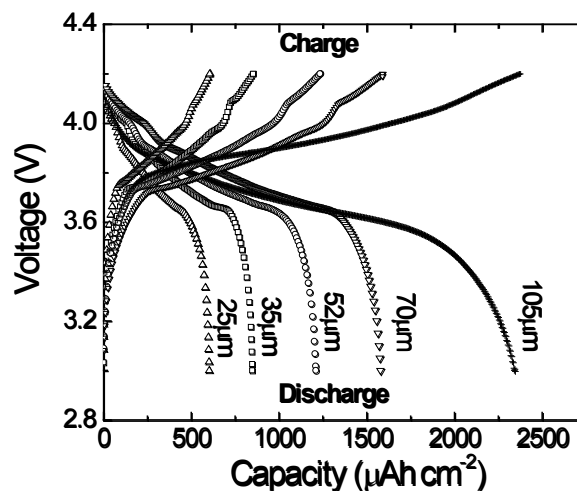


Fig. 5. Discharge capacity curves (5th cycle) for Li-ion microbatteries ($\text{LiCoO}_2/\text{GPE}/\text{MCMB}$) with laser-printed LiCoO_2 cathode films (25, 35, 52, 70 and 105 μm). The active electrode area is 0.49 cm^2 . Batteries were charged at a constant current of 100 $\mu\text{A}/\text{cm}^2$. Based on the theoretical capacities of the LiCoO_2 cathode ($\text{Li}_{0.5}\text{CoO}_2$: $\sim 140 \text{mAh}/\text{g}$) and the MCMB anode (LiC_6 : $\sim 370 \text{mAh}/\text{g}$), all microbatteries tested in this plot were cathode limited.

3.2 Laser structuring

Laser-printed LiCoO_2 thick films were further treated with laser structuring process using a KrF excimer laser in order to increase active surface area of the films for improving Li-ion diffusivity. In the first experiment the laser ablation conditions, such as laser pulse number and laser fluence, were investigated on the surface morphology of the LiCoO_2 thick films.

Variation of laser pulse number:

The influence of laser pulse number was investigated on the surface morphology of the LiCoO_2 films. For this purpose an area of 200 x 200 μm^2 was exposed to the laser beam with a fixed laser fluence of 1.5 J/cm^2 . Figure 6 shows SEM images of laser structured LiCoO_2 thick films as a function of laser pulse number (N). After 100 laser pulses, surface melting is visible and formation of self-organizing surface structures is initiated with structure heights of several micrometers. For N = 200 pulses distinct micron-sized conical surface structures become visible. With further increasing the pulse number (N = 500 and 1000) the number of conical structures is reduced and the

height of the cones is significantly increased. At a pulse number of $N=1000$ the aluminum substrate is exposed locally.

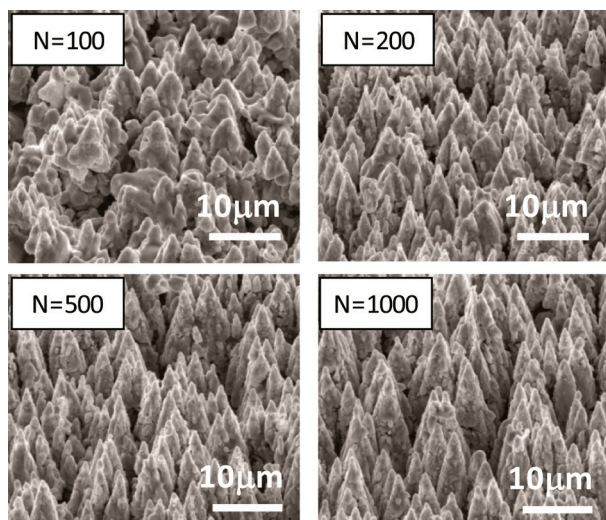


Fig. 6. SEM images of laser structured LiCoO_2 electrode with different laser pulse numbers (N). A KrF excimer laser ($\lambda = 248 \text{ nm}$) was used to apply an energy density of 1.5 J/cm^2 with a pulse width of 5 ns and a laser repetition rate of 100 Hz .

Variation of laser fluence:

The laser fluence was observed to strongly affect the development of the self-organizing structures. Figure 7 shows SEM images of unstructured and laser structured LiCoO_2 electrodes. It can be seen that for a laser fluence of 1.0 J/cm^2 the height of the conical structures is in the range of about $5 \mu\text{m}$. An increase of laser fluence leads to an increase in cone height. The height of the structures reaches values in the range of the film thickness ($\sim 35 \mu\text{m}$) for a laser fluence of 1.5 J/cm^2 . Furthermore, with increasing laser fluence the density of the conical structures is decreased. At a laser fluence of 2.0 J/cm^2 a significant amount of material is clearly ablated, leading to a sizeable loss in active material and substrate exposure. Therefore, a laser fluence of 1.5 J/cm^2 seems as suitable compromise between cone height, structure density and loss of active mass.

Electrochemical Analysis:

Electrochemical cycling was performed to investigate the influence of the laser-structured micro-structures on the electrochemical performance. Figure 8 shows the cycling performance of the unstructured and laser-structured LiCoO_2 cathode films at a constant current between 3.0 V and 4.2 V with a lithium metal anode and a liquid electrolyte of 1M LiPF_6 in ethylene carbonate/ dimethyl carbonate. A constant charge/discharge rate of $C/5$ was applied. The initial discharge capacities obtained are in the range of $100 - 110 \text{ mAh/g}$. Although the unstructured electrode shows slightly higher starting capacities the laser structured cathodes exhibits improved capacity retention. After 25 cycles the capacities of both films reach to the identical value of $\sim 90 \text{ mAh/g}$. At the end of the testing procedure (100 cycles) the laser structured electrodes showed a capac-

ity of $\sim 70 \text{ mAh/g}$, which was twice the remaining capacity of the unstructured cathode.

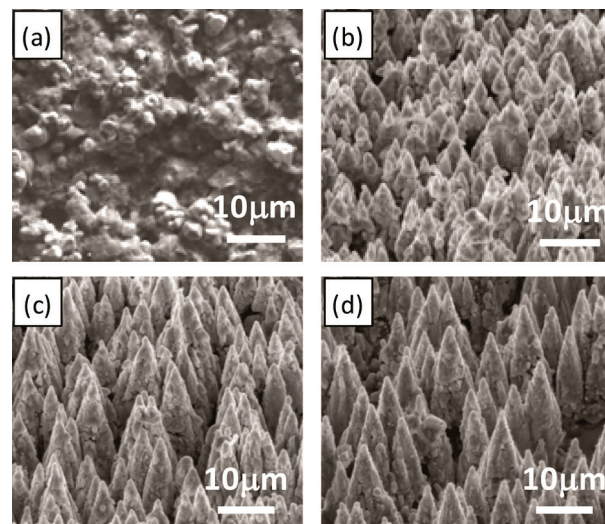


Fig. 7. SEM images of unstructured LiCoO_2 cathode film (a) and laser structured LiCoO_2 films with various laser fluencies of 1.0 J/cm^2 (b), 1.5 J/cm^2 (c), and 2 J/cm^2 (d). A laser pulse number was fixed at 1000 with a pulse width of 5 ns and a laser repetition rate of 100 Hz .

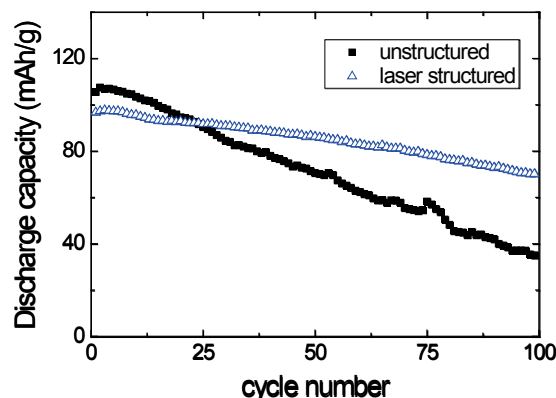


Fig. 8. Cycling performance of unstructured and laser structured LiCoO_2 cathode films. A laser fluence of 1.5 J/cm^2 , laser repetition rate of 300 Hz and laser pulse number of 250 were used for laser structuring.

4. Summary

Thick-film electrodes (LiCoO_2 cathode and MCMB anode) are printed by laser direct write technique and used to fabricate Li-ion microbatteries with gel polymer electrolyte. Battery performance suggests that microbatteries fabricated with these laser-printed thick-film electrodes provide a significantly higher discharge capacity compared to microbatteries based on the sputter-deposited thin films. This increased performance is due to the porous structure of the laser-printed electrodes that allows improved ionic and electronic transport through the thick electrodes without a significant increase in internal cell resistance. The laser-printed LiCoO_2 cathode thick films are further treated by laser structuring process for increasing active surface area

of the films. Preliminary results on battery performance demonstrate that the laser-structured cathode films exhibit an improved capacity retention compared to the unstructured cathode films.

Acknowledgments

This work was supported by the Office of Naval Research. Finally, the support by the Karlsruhe Nano Micro Facility (KNMF, www.kit.edu/knmf) for laser processing is gratefully acknowledged.

References

- [1] J. B. Bates, N.J. Dudney, B. Neudecker, A. Ueda, and C.D. Evans, *Solid State Ion.* **135** (2000) 33.
- [2] N.J. Dudney and Y.-I. Jang, *J. Power Sources* **119-121** (2003) 300.
- [3] B.J. Neudecker, N.J. Dudney, and J.B. Bates, *J. Electrochem. Soc.* **147** (2000) 517.
- [4] Y. Iriyama, M. Inaba, T. Abe, Z. Ogumi, *J. Power Sources* **94** (2001) 175.
- [5] W.-G. Choi and S.-G. Yoon, *J. Power Sources* **125** (2004) 236.
- [6] Y.H. Rho, K. Kanamura, M. Fujisaki, J. Hamagami, S. Suda, T. Umegaki, *Solid State Ionics* **151** (2002) 151.
- [7] A. Piqué, R. C. Y. Auyeung, H. Kim, K. M. Metkus, and S. A. Mathews, *J. Laser Micro/Nanoeng* **3** (2008) 163.
- [8] H. Kim, J. S. Melinger, A. Khachatryan, N. A. Charipar, R. C. Y. Auyeung, and A. Piqué, *Opt. Lett.* **35** (2010) 4039.
- [9] H. Kim, R. C. Auyeung, S. H. Lee, A. L. Huston, and A. Piqué, *J. Phys. D: Appl. Phys.* **43** (2010) 085101.
- [10] H. Kim, R. C. Y. Auyeung, and A. Piqué, *J. Power Sources* **165** (2007) 413.
- [11] T.E. Sutto, M. Ollinger, H. Kim, C.B. Arnold, and A. Piqué, *Electrochemical and Solid-State Letters* **9** (2005) A69.
- [12] H. Kim, R.C.Y. Auyeung, M. Ollinger, G.P. Kushto, Z.H. Kafafi, and A. Piqué, *Appl. Phys. A* **83** (2006) 73.
- [13] R. Wartena, A.E. Curtright, Craig B. Arnold, A. Piqué, K.E. Swider-Lyons, *J. Power Sources* **126** (2004) 193.
- [14] R. W. Hart, H. S. White, B. Dunn, and D. R. Rolison, *Electrochemistry Communications* **5** (2003) 120.
- [15] J. W. Long, B. Dunn, D. R. Rolison, and H. S. White, *Chemical Reviews* **104** (2004) 4463.
- [16] J. F. M. Oudenhoven, L. Baggetto and P. H. L. Notten, *Adv. Energy Mater.* **1** (2011) 10.
- [17] C. L. Wang, L. Taherabadi, G. Y. Jia, M. Madou, Y. T. Yeh, and B. Dunn, *Electrochemical and Solid State Letters* **7** (2004) A435.
- [18] B. Dunn, C. J. Kim, and S. Tolbert, "Three-dimensional microbatteries for MEMS/NEMS technology, in Proceedings of the IEEE International Conference on Micro Electro Mechanical Systems (MEMS)", ed. by M. Wong and Y. Suzuki, (IEEE, New York, 2010) p. 164.
- [19] W. C. West, J. F. Whitacre, V. White, and B. V. Ratnakumar, *Journal of Micromechanics and Microengineering* **12**,(2002) 58.
- [20] A. V. Jeyaseelan and J. F. Rohan, *Applied Surface Science* **256** (2009) S61.
- [21] P. H. L. Notten, F. Roozeboom, R. A. H. Niessen, and L. Baggetto, *Advanced Materials* **19** (2007) 4564.
- [22] R. Kohler, J. Proell, S. Ulrich, V. Trouillet, S. Indris, M. Przybylski, and W. Pfleging, *Proc. of SPIE* **7202**, Bellingham, (2009) p. 1-11.
- [23] J. Proell, R. Kohler, M. Torge, S. Ulrich, C. Ziebert, M. Bruns, H. J. Seifert, and W. Pfleging, *Applied Surface Science* **257** (2011) 9968.
- [24] R. Kohler, H. Besser, M. Hagen, J. Ye, C. Ziebert, S. Ulrich, J. Proell, and W. Pfleging, *Microsystem Technologies* **17** (2011) 225.
- [25] R. Kohler, J. Proell, M. Bruns, S. Ulrich, H.J. Seifert, W. Pfleging, *Appl. Phys. A*, (2012) accepted for publication.

(Received: June 30, 2012, Accepted: October 16, 2012)